Visualizing Semipermeability of Cell Membrane by a pH-responsive Ratiometric AIEgen

Yuan Gu,[ab] Zheng Zhao,[ab] Guangle Niu,[ab] Han Zhang,[c] Yiming Wang,[ab] Ryan T. K. Kwok,[ab] Jacky W. Y. Lam,[ab] and Ben Zhong Tang*[abc]

In clinical chemotherapy, some basic drugs cannot enter the hydrophobic cell membrane because of ionization in acidic tumor microenvironment, a phenomenon known as ion trapping. In this study, we developed a method to visualize this ion trapping phenomenon by utilizing a pH-responsive ratiometric AIEgen, dihydro berberine (dhBBR). By observing the intracellular fluorescence of dhBBR, we found that non-ionized dhBBR can enter cells easier than ionized forms, which is in accordance with the concept of ion trapping. In addition, dhBBR shows superior anti-photobleaching ability than Curcumin thanks to its AIE property. These results suggest that dhBBR can serve as a bioprobe for ion trapping.

Introduction

All living cells must exchange materials with their extracellular environment in order to keep alive.[1,2] The process of substances entering and out of cells are controlled by cell membrane, a biological membrane consisting of a lipid bilayer with proteins embedding in, which separates interior of cells from their external environment.[3,4] Due to the semipermeable nature of lipid bilayer, cell membrane is permeable to non-ionized (fat-soluble) molecules, while the permeability to ionized (water-soluble) molecules is very limited, a phenomenon commonly known as ion trapping.[5] Partial failure in the cancer chemotherapy of some basic drugs, such as vinca alkaloids and anthracyclines, can be ascribed to ion trapping. The acidic tumor microenvironment prevents the ionized alkaline drugs from accumulating in cancer cells.[5-9] Given that, the study of cell membrane's semipermeability, especially ion trapping, is not only fundamentally interesting, but also valuable in improving the clinical chemotherapeutic efficacy.

Ion trapping is most widely studied by HPLC, a well-developed technology.[5,9-12] Although HPLC enjoy the advantages of high sensitivity and selectivity, it usually brings about thorny issues like high equipment cost, complexity, complicated sample processing, and long runtime. Worse more, the biological sample usually needs to be isolated and homogenized, which makes *in situ* monitoring biological process impossible.[13,14]

Fluorescent technology, with their charming merits of simplicity, high sensitivity, and low background noise, is becoming more and more popular in the biomedical research.[15] Thanks to the enthusiastic endeavors made by scientists, a lot of fluorescent bioprobes have been developed for various applications.[16-19] Drugs with inherent fluorescence make real-time *in situ* tracking of drug molecules *in vivo* or *in vitro* possible, which is of critical importance in pharmaceutical research. However, so far, fluorescent drug as probe for monitoring ion trapping has scarcely been reported in spite of its significance in studying the drug delivery and drug distribution in body. This is partly because it is still difficult to find a drug which shows pH-responsive fluorescence. And it is even more challenging to seek a drug which has different emission behaviors between its non-ionized and ionized forms. What's more, fluorescent probes usually suffer from aggregation-caused quenching (ACQ) effect.[20] In 2001, Tang and co-workers discovered aggregation-induced emission (AIE), which is directly opposite to ACQ.[21] Since then, a variety of AIEgens have been developed for many advanced applications.[22,23] Recently, Tang have put forward natural resources as a new source to explore AIEgens.[24] AIEgens, usually obtained from herbal plants, animals, and other natural resources, have a lot of unique advantages, such as synthesis-free, environmental friendly, pharmaceutically active, etc.[24-26] Previously, we have reported that Berberine Chloride, a natural isoquinoline isolated from Chinese herbal plants, is a rotor-free AIEgen.[24] In this study, dihydro Berberine (dhBBR) that converted from Berberine Chloride by gut microorganisms was found to be a AIEgen with pH sensitivity. More importantly, the highly similar molecular structure of dhBBR as BBR enables it work as a suitable drug-

[a] *Department of Chemical and Biological Engineering, Department of Chemistry, the Hong Kong Branch of Chinese National Engineering Research Center for Tissue Restoration and Reconstruction and Institute for Advanced Study, The Hong Kong University of Science and Technology, Clear Water Bay, Kowloon, Hong Kong 999077, China.*

[b] *HKUST- Shenzhen Research Institute, No. 9 Yuexing 1st RD, South Area Hi-tech Park, Nanshan, Shenzhen 518057 China.*

[c] *Center for Aggregation-Induced Emission, SCUT-HKUST Joint Research Institute, State Key Laboratory of Luminescent Materials and Devices, South China University of Technology, Guangzhou 510640, China.*

† Electronic Supplementary Information (ESI) available: Materials and Methods; ^{1}H NMR and HRMS spectra of compounds; Photophysical data and Imaging data.

like probe for visualizing cell membrane's semipermeability thanks to its ratiometric fluorescence.

Results and discussion

Synthesis and photophysical properties

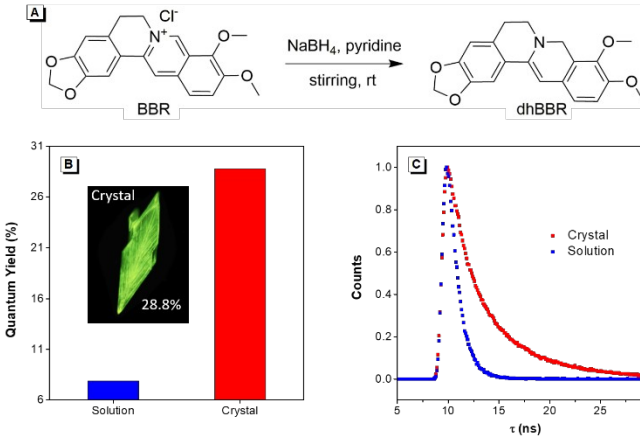

Fig. 1 (A) Synthetic route to dhBBR. (B) Quantum Yield of dhBBR in DMSO solution (10 μM), single crystal, and powder states. Excitation wavelength: 365 nm. (C) Time-resolved emission decay curves of dhBBR in DMSO solution, single crystal, and powder states. Solution concentration: 10 μM; Excitation wavelength: 365 nm.

dhBBR was synthesized according to the route shown in Fig. 1A with 86% yield.[27] The purity of the product was confirmed by ^{1}H NMR as well as high resolution mass spectroscopy (HRMS) (Fig. S1, S2 in ESI). The photoluminescence quantum yield (PLQY) of dhBBR in DMSO solution and crystal states were measured to be 7.9% and 28.8%, respectively (Fig. 1B). The results indicate that dhBBR is a strong solid-state emitter. The fluorescence lifetime of dhBBR in the crystal state (4.68 ns) is longer than that in the solution state (1.1 ns) (Fig. 1C). In addition, from solution to crystal state, the non-radiative decay rate decreases about 5.5 times ($K_{nr,soln}$=8.37 × 10^8 s^{-1}, $K_{nr,crystal}$=1.52 × 10^8 s^{-1}), which should be responsible for the AIE property of dhBBR.

Mechanism study

To have a clear picture on the photophysical properties of dhBBR. The single-crystal structure of dhBBR was analyzed.[28] As shown in Fig. 2, the conformation of dhBBR in crystal is non-planar with a 27.94° twisted angle, which indicates that intramolecular vibration is possible. In addition, the intermolecular distance of adjacent dhBBR molecule aligned in parallel was measured to be 3.771 Å, which exceeds the effective π–π stacking distance (3.5 Å) to quench the fluorescence.[29] What's more, multiple intermolecular interactions (2.408-2.888 Å in distance) contribute to rigidify the molecular conformation which makes dhBBR highly emissive in the crystal. Thus, the brighter emission of dhBBR in crystal than that in solution can possibly be explained by the restriction of intramolecular vibration which suppresses the non-radiative decay pathway.[30] To further clarify the intramolecular

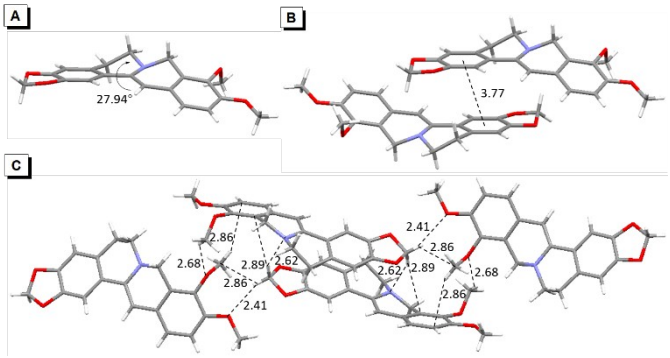

Fig. 2 Single crystal packing of dhBBR.

vibration in determining the photophysical properties of dhBBR, viscosity- and temperature-dependent fluorescence changes of dhBBR were investigated. As shown in Fig. S3(A and B), dhBBR shows stronger emission in viscous solvents or at low temperature because the intramolecular vibration is suppressed.

pH-dependent ratiometric fluorescent response

The nitrogen atom in the molecular backbone of dhBBR is speculated to be protonated in acid.[31,32] As shown in Fig. 3A, dhBBR exhibits obvious pH-dependent fluorescence. Adding acid into dhBBR causes a gradual blue shift of dhBBR's emission from 511 nm to 454 nm as shown in Fig. 3A. To understand dhBBR's pH-dependent fluorescence, absorption titration experiment is performed. As shown in Fig. S4, there is a red shift of the maximum absorption band of dhBBR from 350 nm to 426 nm when the pH of the buffer was changed from 2 to 9. ^{1}H NMR titration study was performed by adding trifluoroacetic acid (TFA) into dhBBR. As shown in Fig. S5, there are downfield shifts of the isoquinoline protons induced by TFA. The new peak at 8.0 suggested that the nitrogen atom in the isoquinoline is protonated. pH titration experiment was then conducted. The fluorescence maximum of dhBBR exhibited a gradual red shift when the pH increased from 1 to 12 (Fig. 3B). More importantly, dhBBR showed an excellent linearity of I_{511}/I_{454} in the pH range of 7-10 with a pKa value of 8.4 (Fig. 3C), which indicated that dhBBR can serve as a ratiometric pH probe. Furthermore, dhBBR showed a good reversibility between pH 2 and pH 12 as shown in Fig. 3D. In addition, the intensity ratios (I_{511}/I_{454}) of dhBBR in pH 3 and pH 10 buffers keep nearly unchanged after 10 min (Fig. S6). The fluorescence response of dhBBR towards different interfering species was evaluated (Fig. 3E). The intensity ratio (I_{511}/I_{454}) was neglectively affected by common metal ions (Na^+, K^+, Ca^{2+}, Mg^{2+}, Fe^{2+}, Cu^{2+}, Zn^{2+}, Mn^{2+}, Al^{3+}, Pb^{2+}, 0.1 mM for Na^+, K^+, Ca^{2+}, Mg^{2+}, 0.01 mM for Fe^{2+}, Cu^{2+}, Zn^{2+},

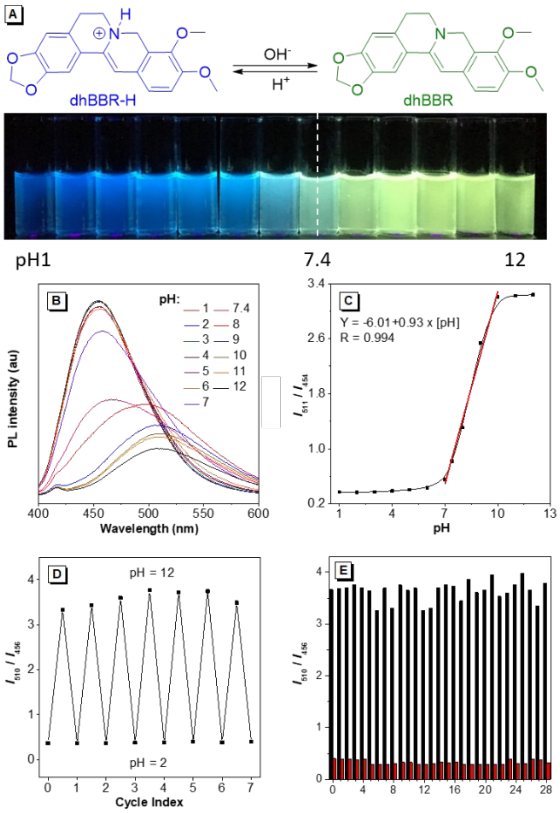

Fig. 3 (A) Schematic illustration of dhBBR's fluorescent response to pH Change. (B) Emission spectra of dhBBR in the PBS buffer solutions with different pH values. [dhBBR] = 10 μM. (C) Plot of I_{511}/I_{454} versus pH. I_{511} and I_{454} denote the emission intensities of the solution at 511 and 454 nm, respectively. Excitation wavelength: 365 nm. (D) Fluorescence reversibility of dhBBR in PBS buffer between pH 2.0 and pH 12.0. [dhBBR] = 10 μM. (E) Ratiometric fluorescent responses of dhBBR (10 μM) to different potential interfering agents in pH 3.0 (red column) and 10.0 (black column) PBS buffer solutions: (0) control; (1) Na^+; (2) K+; (3) Ca^{2+}; (4) Mg^{2+}; (5) Fe^{2+}; (6) Cu^{2+}; (7) Zn^{2+}; (8) Mn^{2+}; (9) Al^{3+}; (10) Pb^{2+}; (11) Ac^-; (12) SO_4^{2-}; (13) NO_3^-; (14) PO_4^{2-}; (15) $S_2O_3^{2-}$; (16) CO_3^{2-}; (17) Phe; (18) His; (19) Met; (20) Pro; (21) Arg; (22) Asp; (23) Cys; (24) Hcy; (25) GSH; (26) Glucose; (27) H_2O_2; (28) NaClO. Conditions: λ_{ex} = 365 nm.

Mn^{2+}, Al^{3+}, Pb^{2+}), negetively charged species (Ac^-, SO_4^{2-}, NO_3^-, PO_4^{2-}, $S_2O_3^{2-}$, CO_3^{2-}, 0.01 mM for SO_4^{2-}, PO_4^{2-}, $S_2O_3^{2-}$, CO_3^{2-}, 0.02 mM for Ac^-, NO_3^-), amino acids (Phe, His, Met, Pro, Arg, Asp, Cys, Hcy, 0.01 mM for each), GSH (0.01 mM), Glucose (0.01 mM), as well as reactive oxygen species (H_2O_2, 0.01 mM; NaClO, 0.01 mM).

Visualizing semipermeability of cell membrane

The ratiometric fluorescent response of dhBBR towards pH and the pharmacological properties of dhBBR[33,34] inspired us to further explore the potential of dhBBR to be utilized as a probe for ion trapping. Before such an exploration, the biocompatibility of dhBBR towards various cell lines was investigated first. As shown in Fig. S7, dhBBR imposes little toxicity towards different cell types at a concentration of 1 μM (with more than 80% cells alive), indicating the feasibility of cell imaging study. For cell imaging, being different from the reported pH-responsive probes which usually used nigericin and monensin for intracellular pH calibration,[35-38] we don't use any chemicals to calibrate intracellular pH because we want intracellular pH to be constant. Instead, we incubated cells with dhBBR-containing PBS buffer of varied pH (pH from 4 to 7.4) for a period. Cells were then imaged under confocal microscopy. It was intriguing to notice that A549 cells incubated with dhBBR-containing PBS of a pH range of 4-6 show almost no emission from both blue and green channels (blue channel: 400-460 nm; green channel: 500-600 nm) (Fig. 4A). In contrast, obvious green fluorescence was observed inside cells when A549 cells were incubated with dhBBR-containing PBS buffer of a pH 7.4 (Fig. 4A). Also, increasing the pH of the PBS buffer from 4 to 7.4 can also induced a gradual increase of emission ratio (I_{Green} / I_{Blue}) (Fig. 4B). Similar results were also observed in HEK 293T cells (Fig. 4C and D). Additionally, different concentrations of dhBBR were used and similar results were obtained in HeLa cells (Fig. S8). This "acid out, base in" phenomenon can be ascribed to the semipermeability of cell membrane as mentioned above. Due to the hydrophobic nature of cell membrane, it makes non-ionized dhBBR easier to enter into cells compared to ionized forms, a phenomenon known as "ion trapping", which well explains why incubating cells with dhBBR-containing PBS of higher pH value causes stronger intracellular fluorescence than dhBBR-containing PBS with lower pH value. Photostability is an important parameter in evaluating a bio-probe's anti-photobleaching ability. As shown in Fig. S10, more than 70% of dhBBR's fluorescence is retained even after 200 seconds of irradiation, while less than 40% of curcumin's fluorescence is retained after the same irradiation time, suggesting that dhBBR has superior anti-photobleaching ability than curcumin thanks to its AIE property.

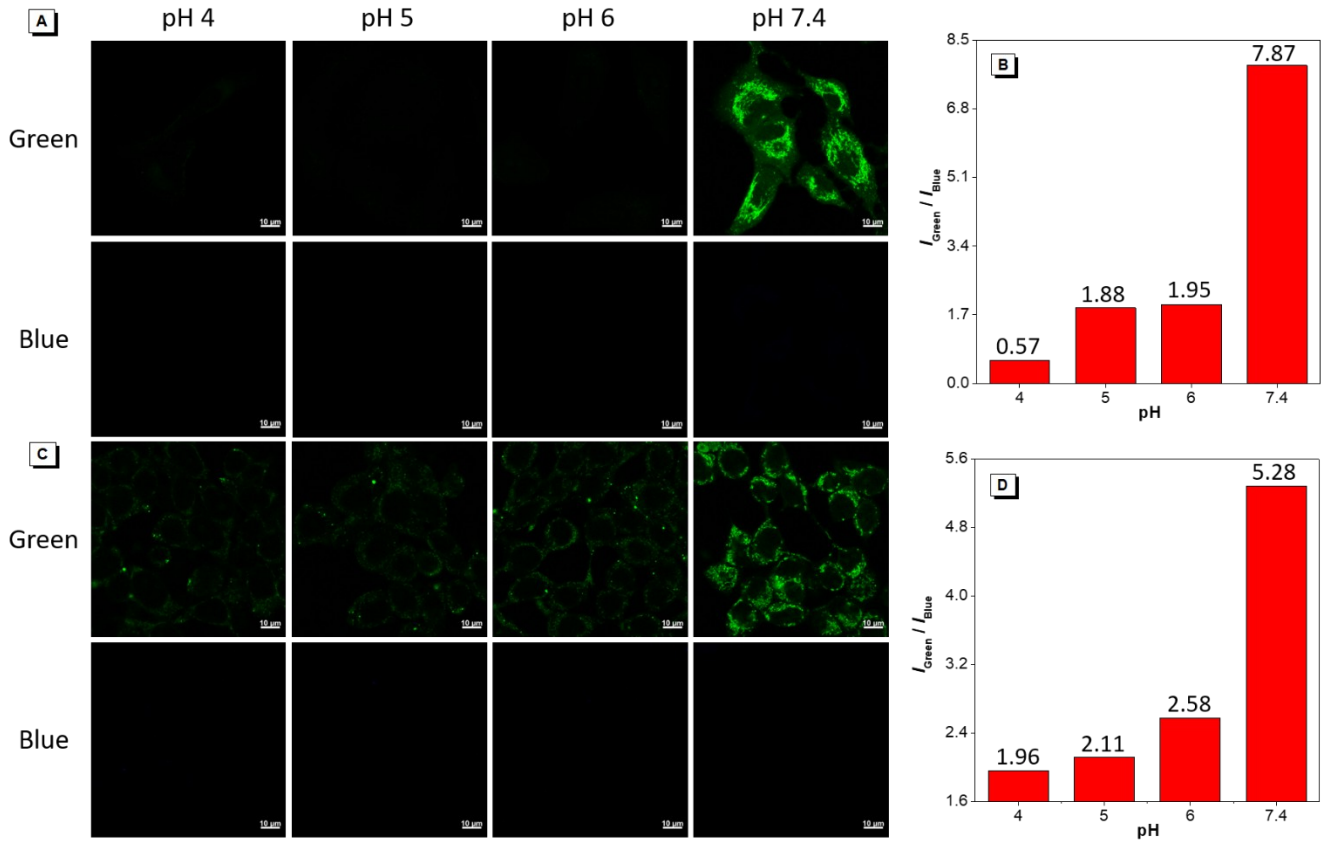

Fig. 4 CLSM images of A549 cells (A) and HEK 293T cells (C) stained with dhBBR (1 μM) in different pH PBS buffers for 30 min. (B, D) Relative PL intensity of dhBBR treated A549 cells (B) and HEK 293T cells (D). Scale bar = 10 μm.

Conclusions

In summary, dihydro berberine (dhBBR) was found to be a AIEgen. Single crystal analysis, viscosity effect, as well as low-temperature effect revealed that the AIE phenomenon of dhBBR originates from the restriction of intramolecular vibration (RIV). Moreover, dhBBR can serve as a fluorescent probe for visualizing ion trapping thanks to its ratiometric fluorescent responses to pH and superior anti-photobleaching ability.

Experimental procedures

Materials and instrumentation

Chemicals for synthesis were purchased from Sigma-Aldrich or Meryer used as received without any further purification. Dihydro Berberine was prepared according to the reported literature.[39] ^{1}H-NMR spectrum was carried out on a Bruker AV 400 spectrometer. High resolution mass spectra (HRMS) were recorded on a GCT premier CAB048 mass spectrometer operating in MALDI-TOF mode. Ultraviolet–visible (UV-vis) absorption spectra were taken on a PerkinElmer Lambda 25 UV-Vis absorption spectrophotometer. Photoluminescence spectra were recorded on a PerkinElmer LS 55 fluorescence spectrometer. The absolute fluorescence quantum yields were measured on a Hamamatsu Absolute Quantum Yield Spectrometer C11347.

Synthesis of dihydro berberine (dhBBR)

Anhydrous Berberine hydrochloride (1 mmol, 371.8 mg) and sodium borohydride (1 mmol, 37.8 mg) were dissolved in pyridine, and then the mixture was stirring slowly at room temperature. After that, ice water was added into the system. The obtained light yellow powdery solid was filtered, dried *in vacuo* to afford pure dhBBR (290.1 mg, 86%). ^{1}H NMR (400 MHz, $CDCl_3$, 25 °C), δ (ppm): 7.14 (1H), 6.71 (2H), 6.55 (1H), 5.92 (3H), 4.29 (2H), 3.82 (6H), 3.12-3.09 (2H), 2.87-2.84 (2H); HRMS (MALDI-TOF, *m/z*): $[M]^+$ calcd. for $C_{20}H_{19}NO_4$, 337.1314; found, 337.1320.

Spectral measurement

The absorption and emission spectra were measured in PBS buffer solutions (10 mM). A stock solution of dhBBR (1 mM) was prepared in DMSO and was subsequently diluted to prepare 10 μM solutions of dhBBR in PBS buffers with various pH (1, 2, 3, 4, 5, 6, 7, 7.4, 8, 9, 10, 11, 12). PBS buffers (10 mM) with varied pH were prepared by using NaOH (1.0 M) or HCl (1.0 M) to adjust the pH. For the calibration curve, 20 μL of stock solutions of dhBBR (1 mM) were mixed with 980 μL different pH of PBS buffers in a quartz optical cell with 1.0-cm optical path length at 25 °C, and spectral data were recorded immediately. Excitation was at 365 nm and emission was detected at 454 nm and 511 nm.

Cell culturing

HeLa cells, A549 cells, and HEK 293T cells were purchased from ATCC. All cells were cultured in Dulbecco's Modified

Eagle's Medium with 1% penicillin-streptomycin and 10% FBS, at 37 °C in a humidified incubator with 5% CO_2. The culture medium was replaced every second day. By treating with 0.25% trypsin-EDTA solution, the cells were collected after they reached confluence.

Cytotoxicity assay

HeLa cells, A549 cells, and HEK 293T cells were seeded in 96-well plates at a density of 5000 cells per well, respectively. After 24 h cell culture, various concentrations of dhBBR were added into the 96-well plate. After another 24 h cell culture, the medium was removed and the freshly prepared MTT medium solution (0.5 mg mL^{-1}, 100 μL) was added into the 96-well plate. After incubation at 37 °C, 5% CO_2 for 6 h, the MTT medium solution was removed carefully. After that, 100 μL DMSO was added into each well and the plate was gently shaken at room temperature to dissolve all the formed precipitates. A microplate reader was utilized to measure the absorbance at 570 nm from which the cell viability could be determined. Cell viability was expressed by the ratio of absorbance of the cells incubated with dhBBR solution to that of the cells incubated with culture medium only.

Cell imaging

Cells were grown in a 35 mm Petri dish with a cover slip at 37 °C, 5% CO_2. Firstly, Cells were incubated with different pH buffers containing dhBBR (0.5, 1, 10 μM) or curcumin (10 μM) for 30 min at 37 °C, 5% CO_2. Then, the staining solution was removed and the cells were washed with PBS of the same pH with the staining solution for three times. After that, the cells were imaged using a confocal microscopy (Zeiss laser scanning confocal microscope LSM7 DUO). For dhBBR, the excitation wavelength was 405 nm, and the emission filter was 400-460 nm and 500-600 nm, respectively; for Curcumin, the excitation wavelength was 405 nm, and the emission filter was 500-600 nm.[40]

Photobleaching assay

HeLa cells stained with dhBBR were irradiated by 405 nm laser for 200s continuously using a confocal microscopy to evaluate dhBBR's photostability. For comparison, HeLa cells stained with Curcumin were irradiated by 405 nm laser under the same conditions.

Conflicts of interest

There are no conflicts to declare.

Acknowledgements

This work was partially supported by the National Natural Science Foundation of China (21788102), the Research Grants Council of Hong Kong (16305518, N-HKUST609/19, A-HKUST605/16, and C6009-17G), the Innovation and Technology Commission (ITC-CNERC14SC01) and the Shenzhen Science and Technology Program (JCYJ20180507183832774). We also thank the technical support from AIEgen Biotech Co., Ltd.

Notes and references

1 P. Marrack, D. Lo, R. Brinster, R. Palmiter, L. Burkly, R. H. Flavell and J. Kappler, *Cell*, 1988, **53**, 627–634.
2 R. Sutherland, *Science*, 1988, **240**, 177–184.
3 K. Simons and E. Ikonen, *Nature*, 1997, **387**, 569–572.
4 S. J. Singer and G. L. Nicolson, *Science*, 1972, **175**, 720–731.
5 N. Raghunand, B. P. Mahoney and R. J. Gillies, *Biochem. Pharmacol.*, 2003, **66**, 1219–1229.
6 H. Arnold, F. Bourseaux and N. Brock, *Nature*, 1958, **181**, 931–931.
7 B. A. Webb, M. Chimenti, M. P. Jacobson and D. L. Barber, *Nat. Rev. Cancer*, 2011, **11**, 671–677.
8 F. Lucien, P.-P. Pelletier, R. R. Lavoie, J.-M. Lacroix, S. Roy, J.-L. Parent, D. Arsenault, K. Harper and C. M. Dubois, *Nat. Commun.*, 2017, **8,** 15884.
9 N. Raghunand and R. J. Gillies, *Drug Resist. Updates*, 2000, **3**, 39–47.
10 M. K. Nair, D. J. Chetty, Y. W. Chien and H. Ho, *J. Pharm. Sci.*, 1997, **86**, 257–262.
11 L.-L. H. Chen, D. J. Chetty and Y. W. Chien, *Int. J. Pharm.*, 1999, **184**, 63–72.
12 H. M. Nielsen and M. R. Rassing, *Eur. J. Pharm. Sci.*, 2002, **16**, 151–157.
13 C. Yin, F. Huo, J. Zhang, R. Martínez-Máñez, Y. Yang, H. Lv and S. Li, *Chem. Soc. Rev.*, 2013, **42**, 6032-6059.
14 S. Wang, H. Yin, Y. Huang and X. Guan, *Anal. Chem.*, 2018, **90**, 8170–8177.
15 C. Caskey, *Science*, 1987, **236**, 1223–1229.
16 R. Wirth, P. Gao, G. U. Nienhaus, M. Sunbul and A. Jäschke, *J. Am. Chem. Soc.*, 2019, **141**, 7562–7571.
17 C. J. Macnevin, T. Watanabe, M. Weitzman, A. Gulyani, S. Fuehrer, N. K. Pinkin, X. Tian, F. Liu, J. Jin and K. M. Hahn, *J. Am. Chem. Soc.*, 2019, **141**, 7275–7282.
18 Q. Qi, W. Chi, Y. Li, Q. Qiao, J. Chen, L. Miao, Y. Zhang, J. Li, W. Ji, T. Xu, X. Liu, J. Yoon and Z. Xu, *Chem. Sci.*, 2019, **10**, 4914–4922.
19 H. Y. Kwon, X. Liu, E. G. Choi, J. Y. Lee, S. Y. Choi, J. Y. Kim, L. Wang, S. J. Park, B. Kim, Y. A. Lee, J. J. Kim, N. Y. Kang and Y. T. Chang, *Angew. Chem., Int. Ed.,* 2019, **58**, 8426-8431.
20 M. Yamaguchi, S. Ito, A. Hirose, K. Tanaka and Y. Chujo, *Mater. Chem. Front.*, 2017, **1**, 1573–1579.
21 C. Zhu, R. T. K. Kwok, J. W. Y. Lam and B. Z. Tang, *ACS Appl. Bio Mater.*, 2018, **1**, 1768–1786.
22 J. Mei, N. L. C. Leung, R. T. K. Kwok, J. W. Y. Lam and B. Z. Tang, *Chem. Rev.,* 2015, **115**, 11718–11940.
23 R. T. K. Kwok, C. W. T. Leung, J. W. Y. Lam and B. Z. Tang, *Chem. Soc. Rev.,* 2015, **44**, 4228–4238.
24 Y. Gu, Z. Zhao, H. Su, P. Zhang, J. Liu, G. Niu, S. Li, Z. Wang, R. T. K. Kwok, X.-L. Ni, J. Sun, A. Qin, J. W. Y. Lam and B. Z. Tang, *Chem. Sci.*, 2018, **9**, 6497–6502.
25 B. Li, X. Xie, Z. Chen, C. Zhan, F. Zeng and S. Wu, *Adv. Funct. Mater.*, 2018, **28**, 1800692.
26 T. He, N. Niu, Z. Chen, S. Li, S. Liu and J. Li, *Adv. Funct. Mater.*, 2018, **28**, 1870068.
27 S. Fu, Y. Xie, J. Tuo, Y. Wang, W. Zhu, S. Wu, G. Yan and H. Hu, *MedChemComm*, 2015, **6**, 164–173.
28 K. Biradha, *CrystEngComm*, 2003, **5**, 388-391.
29 M. D. Curtis, J. Cao and J. W. Kampf, *J. Am. Chem. Soc.*, 2004, **126**, 4318–4328.
30 N. L. C. Leung, N. Xie, W. Yuan, Y. Liu, Q. Wu, Q. Peng, Q. Miao, J. W. Y. Lam and B. Z. Tang, *Chem. - Eur. J.*, 2014, **20**, 15349–15353.
31 W. Adam, A. Grimison and G. Rodríguez, *Tetrahedron*, 1967, **23**, 2513–2521.
32 G. A. Olah, A. M. White and D. H. Obrien, *Chem. Rev.*, 1970, **70**, 561–591.
33 R. Feng, J.-W. Shou, Z.-X. Zhao, C.-Y. He, C. Ma, M. Huang, J. Fu, X.-S. Tan, X.-Y. Li, B.-Y. Wen, X. Chen, X.-Y. Yang, G.

Ren, Y. Lin, Y. Chen, X.-F. You, Y. Wang and J.-D. Jiang, *Sci. Rep.*, 2015, **5**, 12155.
34 D. Yu, L. Lv, L. Fang, B. Zhang, J. Wang, G. Zhan, L. Zhao, X. Zhao and B. Li, *Plos One*, 2017, **12**(8), e0181823.
35 X. Liu, Y. Su, H. Tian, L. Yang, H. Zhang, X. Song and J. W. Foley, *Anal. Chem.*, 2017, **89**, 7038–7045.
36 K. Li, Q. Feng, G. Niu, W. Zhang, Y. Li, M. Kang, K. Xu, J. He, H. Hou and B. Z. Tang, *ACS Sens.*, 2018, **3**, 920–928.
37 G. Niu, P. Zhang, W. Liu, M. Wang, H. Zhang, J. Wu, L. Zhang and P. Wang, *Anal. Chem.*, 2017, **89**, 1922–1929.
38 J. Zhang, M. Yang, W. Mazi, K. Adhikari, M. Fang, F. Xie, L. Valenzano, A. Tiwari, F.-T. Luo and H. Liu, *ACS Sens.*, 2015, **1**, 158–165.
39 S. Fu, Y. Xie, J. Tuo, Y. Wang, W. Zhu, S. Wu, G. Yan and H. Hu, *MedChemComm*, 2015, **6**, 164–173.
40 A. Kunwar, A. Barik, B. Mishra, K. Rathinasamy, R. Pandey and K. Priyadarsini, *Biochim. Biophys. Acta*, 2008, **1780**, 673–679.